

Response to comment of BGD-12-C182-2015

Comment of Referee #1:

The research implemented a very unique N₂O sampling network consisting of 147 sampling locations on a single field of 4 ha of tea. This level of sampling requires an extraordinary effort, and the data so obtained are of unique value for evaluating spatial variability of N₂O emissions from agricultural soils. The manuscript is worth publishing.

Author's Response:

We highly appreciated the encouragement made by the referee #1.

Author's Changes to the Manuscript:

No change.

Response to comment of BGD-12-C194-2015

Comment of Referee #2:

This paper by Fu et al. reports a study on the spatial variability of N₂O emissions from a tea field during the wet season in subtropical China. The authors measured N₂O emissions using 147 chambers and applied three spatial interpolation methods to estimate the spatial distribution of the emissions. The findings highlight the importance of selecting an appropriate spatial interpolation method to provide a reliable estimation of regional N₂O emissions.

The paper makes a contribution to knowledge. The methodology is sound and the conclusions are supported by the results. The paper is well written and deserves publication.

Just one minor edit: P.1488, L14: change “The” to “the”.

Author’s Response:

We highly appreciated the encouragement made by the referee #2, and many thanks for the minor comment. We made the correction in the revised manuscript.

Author’s Changes to the Manuscript:

See change in P.18, L377 in the revised manuscript.

Responses to comments of BGD-12-C456-2015

Comment I of the Editor:

I.1) Please elaborate in detail the major novelty of this paper compared to the study from Li et al., 2013. Simply referring to dry season in one paper and to wet season in the other is not sufficient.

I.2) In addition, comparing dry and wet season should be done carefully as half an hour sampling cannot represent an entire season.

I.3) It is suggested in the abstract that soil properties should be included in interpolation methods. To my opinion, such an achievement would be required before final publication.

Author's Response:

I.1) In subtropical central China, the temperature and precipitation are very different between wet season and dry season as well as subsequent field management, e.g., fertilization and weeding, which may result in strong seasonal variations of N₂O emissions from tea-planted soils with totally different spatial structures and controlling factors. Therefore, this wet season study is a companion investigation of the dry season study (Li et al., 2013) for looking at the spatial variability of N₂O emissions from tea field soils.

Compared to Li et al. (2013), the major novelties in this study may include the following three aspects. Firstly, the sampling chambers were redesigned (please see P8-9 L162-168 of Section 2.3 in the revised manuscript) to be more practical. Basically, the bases and the sampling chambers are separated. When in field operation, the chambers are clipped on the bases with sponge seals in between to stop the gas leaking. Thus, the volume of each sampling chamber is kept almost the same. Secondly, the sampling grids of this study (15 m S-N x 15 m E-W) were slightly denser than the dry-season study (15 m S-N x 20 m E-W). Finally, although we found that the spatial structures of N₂O emissions were comparable during both the dry and wet seasons (with an effective range of approximately 28.0 m and 25.3 m, respectively), the influencing factors of N₂O emissions were quite different, of which soil properties (soil ammonium, soil nitrate and soil organic carbon) and elevation had significant impacts on N₂O emissions during the wet and dry seasons, respectively. In addition, the total amount of N₂O emissions in the wet season was almost seven times

more than that during the dry season for a 30-min snapshot (10:00-10:30 a.m.) over the studied 4.0 ha tea-planted catchment.

I.2) Yes, we agreed that a 30-min measurement cannot fully represent the N₂O emissions for an entire season. However, the main objective of this study was to investigate the spatial structure and controlling factors of N₂O emissions from tea-planted soil, while the seasonal variation of the amounts of N₂O emissions was regarded important, but less concerned.

I.3) Yes, we totally agreed. In the cokriging interpolation approach, soil properties such as soil organic carbon, soil ammonium-N and soil nitrate-N (which had significant correlations with N₂O fluxes) were chosen as the co-variables for estimating the spatial distribution of N₂O emissions (see Sections 3.3 and 4.3 in the revised manuscript).

Author's Changes to the Manuscript:

No change.

Comment II of the Editor:

II) The paper should refer to and discuss process-based biogeochemical modeling approaches (e.g., DNDC). Which implication do the results of the paper have for existing models and process understanding (see e.g., Butterbach-Bahl et al., 2013)?

Author's Response:

The main objective of this paper was to explore the spatial structure and controlling factors of N₂O emissions from tea-planted soils over a catchment. The outcomes of

such a research may help us to design the static chamber positioning scheme when a continuous measurement of N₂O emissions from tea fields is carried out, and provide a more accurate estimation of N₂O emissions at regional scales. Although the main controlling factors of N₂O emissions from tea fields found in this study were helpful for the relationship development, there were few direct contributions to understand the biogeochemical processes simulated in the ecosystem models such as DNDC and DAYCENT.

Author's Changes to the Manuscript:

No change.

Comment III of the Editor:

III) Provide more details on the size of the static chamber (e.g., volume). Please also explain why the chamber volumes were not ventilated (air mixing to avoid concentration gradients)? Could this potentially cause random sampling errors that have influenced the spatial distribution of the emissions?

Author's Response:

The static chambers were divided into two parts: base and chamber. The base was 0.15 m in diameter and 0.05 m high. The chamber was 0.15 m in diameter and 0.15 m high. In the field operation, the base was gently inserted vertically into the soil, and the chamber was clipped on the base with the sponge seals in between to stop gas leaking. Therefore, the effective static chambers volume was equal to the chamber volume of 0.002651 m³.

Theoretically, these static chambers should be ventilated for balancing air pressure at operation. However, our pre-experiment of gas sampling had proven that the ventilation of the chamber had little impact on the N₂O concentration gradients during a short incubation time period of 30-min. Therefore, to avoid the unnecessary complexity of the gas sampling chamber, the ventilation device was not applied in our study.

Author's Changes to the Manuscript:

please see changes in P.8-9, L162-171 of Section 2.3 in the revised manuscript.

Comment IV of the Editor:

IV) It would be important to see the spatial distribution of the error of the interpolation (kriging variance) on a map.

Author's Response:

Yes, we agreed. A new kriging variance map (Fig. 10) for Fig. 9 was produced and its relevant description was also made in the revised manuscript.

Author's Changes to the Manuscript:

The new kriging variance map (Fig. 10) was added in P.49 in the revised manuscript, and the relevant description was added in P.14, L293-294 in Section 3.3 in the revised manuscript. The map caption was also added in P.39 L674-680.

1 Wet-season spatial variability of N₂O emissions from a tea field in subtropical central China

2

3 Xiaoqing Fu, Xinliang Liu, Yong Li *, Jianlin Shen, Yi Wang, Ganghua Zou, Hang Li, Lifang

4 Song, Jinshui Wu

5

6 Changsha Research Station for Agricultural & Environmental Monitoring and

7 Key Laboratory of Agro-ecological Processes in Subtropical Regions,

8 Institute of Subtropical Agriculture, Chinese Academy of Sciences,

9 Hunan 410125, China

10 These two authors contributed equally to this work.

11 *Correspondence to: Professor Yong Li

12 Institute of Subtropical Agriculture,

13 Chinese Academy of Sciences, Hunan 410125, China

14 Tel: +86-731-8461-5291

15 Fax: +86-731-8461-2685

16 E-mail: yli@isa.ac.cn

17

18 **Abstract**

19 Tea fields emit large amounts of nitrous oxide (N₂O) to the atmosphere. Obtaining accurate
20 estimations of N₂O emissions from tea-planted soils is challenging due to strong spatial
21 variability. We examined the spatial variability of N₂O emissions from a red-soil tea field in
22 Hunan province, China, on 22 April 2012 (in a wet season) using 147 static mini chambers
23 approximately regular gridded in a 4.0 ha tea field. The N₂O fluxes for a 30-min snapshot
24 (10:00-10:30 am) ranged from -1.73 to 1,659.11 g N ha⁻¹ d⁻¹ and were positively skewed with
25 an average flux of 102.24 g N ha⁻¹ d⁻¹. The N₂O flux data were transformed to a normal
26 distribution by using a logit function. The geostatistical analyses of our data indicated that the
27 logit-transformed N₂O fluxes (FLUX30t) exhibited strong spatial autocorrelation, which was
28 characterized by an exponential semivariogram model with an effective range of 25.2 m. As
29 observed in the wet season, the logit-transformed soil ammonium-N (NH₄Nt), soil nitrate-N
30 (NO₃Nt), soil organic carbon (SOct), total soil nitrogen (TSNt) were all found to be
31 significantly correlated with FLUX30t ($r=0.57-0.71$, $p< 0.001$). Three spatial interpolation
32 methods (ordinary kriging, regression kriging and cokriging) were applied to estimate the
33 spatial distribution of N₂O emissions over the study area. Cokriging with NH₄Nt and NO₃Nt
34 as covariables ($r=0.74$ and RMSE=1.18) outperformed ordinary kriging ($r=0.18$ and
35 RMSE=1.74), regression kriging with the sample position as a predictor ($r=0.49$ and
36 RMSE=1.55) and cokriging with SOct as a covariable ($r=0.58$ and RMSE=1.44). The
37 predictions of the three kriging interpolation methods for the total N₂O emissions of 4.0 ha
38 tea field ranged from 148.2 to 208.1 g N d⁻¹, based on the 30 min snapshots obtained during

39 the wet season. Our findings suggested that to accurately estimate the total N₂O emissions
40 over a region, the environmental variables (e.g., soil properties) and the current land use
41 pattern (e.g., tea row transects in the present study) must be included in spatial interpolation.
42 Additionally, compared with other kriging approaches, the cokriging prediction approach
43 showed great advantages in being easily deployed, and more importantly providing accurate
44 regional estimation of N₂O emissions from tea-planted soils.

45

46 **Introduction**

47 According to the latest data, which show rapid increases in their atmospheric concentrations
48 ([IPCC, 2013](#)), nitrous oxide (N₂O), carbon dioxide (CO₂) and methane (CH₄) are three major
49 greenhouse gases in the atmosphere that significantly contribute to global warming. Among
50 these major greenhouse gases, N₂O has a very high radiative forcing per unit mass (265-fold
51 stronger than CO₂ on a 100 year horizon) and plays an important role in ozone depletion in
52 the stratosphere ([Ravishankara et al., 2009](#)). The primary sources of N₂O are from agriculture
53 development and the subsequent increased use of chemical N fertilizers ([Ambus and](#)
54 [Christensen, 1994](#); [Mosier et al., 1996, 1998](#); [Yanai et al., 2003](#); [Tokuda and Hayatsu, 2004](#);
55 [Akiyama et al., 2006](#); [Ravishankara et al., 2009](#)). Agricultural soils produce 2.8 (1.7–4.8) Tg
56 of N₂O-N yr⁻¹ ([IPCC, 2013](#)). The N₂O is emitted from soils via the microbial processes of
57 nitrification under aerobic conditions and denitrification under anaerobic conditions
58 ([Firestone and Davidson, 1989](#); [Wrage et al., 2004](#)). The magnitude of soil N₂O emissions is
59 highly variable and strongly influenced by changes in environmental conditions.

60 Among the different agricultural soils, tea-planted soils are important sources of N₂O that
61 are rapidly attracting attention due to recent large increases in the number of tea plantations
62 and large N fertilizer inputs ([Akiyama et al., 2006](#); [Lin and Han, 2009](#); [Fu et al., 2010, 2012](#);
63 [Hirono and Nonaka, 2012](#); [Han et al., 2013](#); [Li et al., 2013](#)). In China, the total tea-planted
64 area was approximately 2.10 million ha (mostly distributed in Fujian, Anhui, Zhejiang and
65 Hunan) in 2013 ([NBSC, 2014](#)). Compared with other agricultural soils, tea-planted soils
66 provide optimal conditions (e.g., low soil pH, high temperature and ample moisture) for
67 microbes to emit significant amounts of N₂O ([Hayatsu, 1993](#); [Venterea and Rolston, 2000](#); [Li](#)
68 [et al., 2013](#)). However, because few measurements of N₂O emissions from tea-planted soils
69 have been reported in China ([Fu et al., 2012](#); [Li et al., 2013](#); [Han et al., 2013](#)), it is difficult to
70 conduct precise spatial and temporal evaluations of N₂O emissions from tea-planted soils. To
71 estimate the N₂O emissions from tea-planted soils accurately and to understand the roles that
72 tea plantations play in global warming, it is necessary to investigate the spatial and temporal
73 patterns and related mechanisms of N₂O emissions from tea fields. This information will lead
74 to the development of effective land management options for mitigating N₂O emissions from
75 a significant source, tea plantation.

76 The N₂O fluxes have large spatial variability in agricultural soils ([Konda et al., 2008](#),
77 [2010](#); [Meda et al., 2012](#); [Li et al., 2013](#)). Many previous studies in tea fields have found
78 pronounced seasonal fluctuations in N₂O fluxes, with higher N₂O emissions during the wet
79 season than during the dry season ([Fu et al., 2012](#); [Han et al., 2013](#)). The seasonal and spatial
80 variability of N₂O emissions significantly contributes to the uncertainty when estimating the

81 contributions of subtropical tea-planted ecosystems to N₂O flux. Moreover, most of our
82 knowledge regarding seasonal changes and the spatial variability of N₂O fluxes is based on a
83 small number of measurements taken from tea-planted soils. [Li et al. \(2013\)](#) investigated the
84 spatial structure of N₂O fluxes for tea-planted soils during the dry season in October 2010
85 and found that the spatial distribution of the N₂O fluxes was primarily associated with field
86 elevation ($r=-0.42$, $p<0.001$). The other soil properties (e.g., soil organic carbon, soil water
87 and soil mineral nitrogen) were not significantly related to N₂O flux. To obtain a more
88 accurate evaluation of annual N₂O emissions from tea-planted soils, a study on the spatial
89 structure and distribution of N₂O emissions during a wet season (in contrast to the dry season)
90 is necessary.

91 To understand the structure of the spatially distributed data and to predict the N₂O fluxes
92 at the unsampled locations, geostatistical analyses can be useful ([Goovaerts, 1997](#); [Webster
93 and Oliver, 2001](#)). Geostatistics provide statistical tools for describing the quantitative spatial
94 variability of field observations for the accurate mapping and planning of rational sampling
95 schemes that efficiently utilize the available labor ([Webster, 1985](#)). Several geostatistical
96 methods are used to examine the spatial variability of N₂O fluxes, including simple kriging
97 (SK), ordinary kriging (OK), regression kriging (RK) and cokriging (CK). The most
98 commonly used method is OK ([Clemens et al., 1999](#); [Röver et al., 1999](#); [Mathieu et al., 2006](#);
99 [Konda et al., 2008, 2010](#)), which uses the derived theoretical semivariogram models to
100 interpolate the spatial distribution of N₂O fluxes. However, research has demonstrated that
101 RK and CK approaches, which use related auxiliary variables, improve the prediction

102 accuracy (Goovaerts, 1997; Webster and Oliver, 2001; Hengl et al., 2004). The RK method
103 combines multiple regressions, including linear regressions, generalized linear models,
104 generalized added models and regression tree models, with the auxiliary variables used for
105 kriging (Odeh et al., 1994). In the RK method, linear regressions are commonly used. The
106 CK approach uses correlations that may exist between the predicted variables and other more
107 easily measured variables. These variables can be measured at the same points as the
108 predicted variable, at other points, or at both. Compared with the RK approach, the CK
109 approach is commonly applied when the measurement of a covariable is less expensive than
110 the cost of a predicted variable (Stein et al., 1988; Odeh et al., 1995). In addition to the
111 feature correlation as a criterion for selecting covariables, the CK approach also requires that
112 both of the predicted variable and covariables have similar spatial structures (Odeh et al.,
113 1994). In this study, we used three interpolation methods (OK, RK and CK) to estimate the
114 spatial distribution of N₂O fluxes in a tea field.

115 In contrast with the dry season, the spatial variability of the N₂O emissions was
116 investigated during the wet season in April 2012 from the same tea-planted catchment that
117 was studied by Li et al. (2013). The catchment consisted of a completely independent
118 hydrological system. Thus, the spatial distribution of the N₂O emissions within the catchment
119 was expected to have intrinsic characteristics. The objectives of this study were to (i) evaluate
120 the spatial variability of N₂O emissions from soils planted with tea in subtropical central
121 China during the wet season, (ii) determine the key environmental factors controlling N₂O
122 emissions, and (iii) assess the prediction efficiency of three kriging interpolation methods.

123

124 **2. Materials and Methods**

125 *2.1 Site description*

126 The field experiment was conducted in a small catchment (4.0 ha) in Jinjing, Changsha, in
127 Hunan province, China (28°32'50"N and 113°19'58" E and elevation 90 to 111 m) (Fig. 1).

128 The region has a subtropical monsoon climate with a mean annual air temperature of 17.5°C
129 and a mean annual precipitation of 1400 mm (average from 1979 to 2012). The site had four
130 distinct seasons: spring (February to April), summer (May to July), autumn (August to
131 November), and winter (December to January). On average, 70% of the annual precipitation
132 occurred in April, May and June. The daily air temperature and precipitation for 2012 were
133 recorded by an automatic weather station (Intelimet A, IMET-ADV2, Dynamax, USA)
134 located next to the studied catchment (Fig. 2). The soil of the catchment was a Haplic Alisol
135 (FAO/UNESCO soil taxonomy) that was derived from a granitic parental material. Tea
136 (*Camellia sinensis L., cv. Baihaozao*) was contour-planted 10 years ago using an inter-row
137 spacing of 0.5 m in the catchment.

138

139 *<Insert Figs. 1 & 2 near here>*

140

141 *2.2 Sampling positions*

142 In the 4.0 ha tea-planted catchment, 1964 evenly-distributed points with plane coordinates
143 and elevation values and 456 centerlines of tea tree row were recorded by locally calibrated
144 differential Geographic Positioning System (DGPS) receiver (Sanding Southern Survey Co.,

145 China), and then were used to develop the local DEM and land use data (at a spatial
146 resolution of 0.1 m, respectively, as shown in Fig. 1c and d). The land use data showed the
147 four positions where the chambers were placed, including the inter-row, fertilization point,
148 under tea tree and in tea tree row, as described in Li. et al. (2013). The spatial positions of the
149 gas sampling points in a 15 m × 15 m regular grid over the catchment were originally
150 determined using a DGPS receiver on 20 April 2012. Some of the chamber positions were
151 slightly adjusted (because of a lack of space in the tea tree rows or to avoid roads and
152 trenches). Thus, the chambers were placed in one of four locations mentioned above (Fig. 1d).
153 Overall, 147 sampling points were determined, and the Euclidean distances between each
154 point and its nearest neighbors ranged from 14.6 m to 16.7 m. The x-y coordinates, the gas
155 sampling position information (the inter-row, fertilization point, under tea tree and in tea tree
156 row along tea row transects), and the elevations at the sampling points were recorded.

157

158 2.3 Gas and soil properties measurements

159 Gas and soil samples were collected at each grid point on 22 April 2012 using a closed mini
160 chamber technique. A mini chamber set was composed of PVC and had two parts (base and
161 chamber). The base was 0.15 m in diameter and 0.05 m high. The chamber was 0.15 m in
162 diameter and 0.15 m high, and was equipped with rubber septa on the top for gas sampling. In
163 the field operation, the base was gently inserted vertically into the soil on 20 April 2012, and
164 the chamber was clipped on the base with the sponge seals in between to stop gas leaking
165 before gas sampling on 22 April 2012. Therefore, the effective static chambers volume was

166 ~~equal to the chamber volume of 0.002651 m³. The mini chambers were composed of PVC and~~
167 ~~had two parts (base and lid). The bases were 0.15 m tall and were gently inserted into the soil~~
168 ~~vertically to a depth of 0.05 m on 20 April 2012. The lids with rubber septa for gas sampling~~
169 ~~were screwed onto the bases when the gas was sampled on 22 April 2012.~~ Gas samples were
170 collected from the headspace between 10:00 and 10:30 am. For simultaneous sampling, 25
171 skilled gas sampling persons helped to accomplish the field sampling. Each person only took
172 care of one column containing 4 to 8 sampling positions (see Fig. 1), and started sampling at
173 the same time of 10 am. At each point, three gas sample replicates were collected from the
174 headspace into pre-evacuated 12 mL vials (Exetainers, Labco, UK) at 0 and 30 min after the
175 chamber body was clipped. After collecting the gas samples, the air temperature in each
176 chamber was measured for subsequent correction of the flux calculation, and then three
177 replicate soil cores, 0.05 m in diameter and 0.20 m in depth, were collected from the soils
178 inside the mini chambers. Soil samples were put straight into clean zip-lock bags for avoiding
179 soil moisture loss, and quickly transported back to the laboratory in thermal insulation boxes
180 and stored in a refrigeration room at 4 °C for preventing any microbial activity (such as
181 mineralization, nitrification and denitrification). The N₂O concentrations of the gas samples
182 were analyzed using a gas chromatograph (Agilent 7890A, Agilent, USA) that was fit with a
183 ⁶³Ni-electron capture detector and an automatic sample injector system. The N₂O fluxes
184 (FLUX30, g N ha⁻¹ d⁻¹) were calculated as described by Li et al. (2013). The soil
185 physical/chemical properties determined by using fresh soil, e.g., the soil ammonium content
186 (NH₄N), soil nitrate content (NO₃N), soil dissolved organic carbon content (DOC), soil

187 volumetric water content (SWC), and soil bulk density (BD), were measured within three
188 days after sampling, while those using air-dried soil, e.g., total soil nitrogen content (TSN),
189 soil organic carbon content (SOC) and soil clay/silt/sand content (CLAY, SILT and SAND),
190 were determined within two weeks after the field work.

191

192 2.4 Data analyses

193 The descriptive statistical and geostatistical analyses were performed using R (R
194 Development Core Team, 2014) with the gstat package (DGUU, 2010).

195 Descriptive statistical analyses were used to determine the mean, median, minimum and
196 maximum values, SD, coefficient of variation (CV), and skewness of the original and
197 logit-transformed data. These analyses were based on the four chamber placement positions.
198 Because the FLUX30, NH4N, NO3N, SOC, TSN and SWC data were highly skewed, these
199 values were transformed by using a logit function (Hengl et al., 2004). The transformed
200 variables were named FLUX30t, NH4Nt, NO3Nt, SOct, TSNt and SWCt. Using a Pearson's
201 correlation, the relationships between FLUX30t, NH4Nt, NO3Nt, SOct, TSNt, SWCt, DOC,
202 BD, SAND, SILT, and CLAY were tested. The significance of the differences in the FLUX30t
203 and environmental factors (NH4Nt, NO3Nt, SOct, TSNt and DOC) between any two of the
204 different chamber positions along the entire tea-tree row transect were evaluated using the
205 Tukey's Honest Significant Difference method.

206 In the geostatistical analyses, an experimental semivariogram of FLUX30t was
207 calculated, and the theoretical semivariogram models were fit. The ratio of the partial sill to

208 the total sill was used as an index of spatial dependence. [Armstrong \(1998\)](#) stated that a
209 variable with a higher ratio of partial sill to sill and a longer semivariogram range were more
210 structured. The spatial distribution of FLUX30t across the catchment was predicted using
211 three kriging interpolation methods (OK, RK and CK). These data were transformed back to
212 the original scale of FLUX30 for mapping. The Leave-One-Out cross-validation method was
213 used to evaluate the accuracy of interpolating FLUX30t using the three different kriging
214 methods.

215

216 **3. Results**

217 *3.1 Exploratory data analyses*

218 In the 4.0 ha tea-planted catchment, the N₂O fluxes during the 30-min one-time
219 measurements performed on 22 April 2012 ranged from -1.73 to 1,659.11 g N ha⁻¹ d⁻¹, with a
220 median value of 27.56 g N ha⁻¹ d⁻¹ and a CV of 234.7 % ([Table 1](#)). The N₂O flux data were
221 positively skewed ([Table 1 and Fig. 3a](#)), and their logit-transformations were approximately
222 normally distributed ([Table 1 and Fig. 3b](#)). From [Table 3](#), the logit-transformed N₂O fluxes
223 (FLUX30t) were the highest in the fertilization points, and the differences in the FLUX30t
224 values among the chamber placement positions were statistically significant ($p < 0.001$).

225

226 *<Insert Table 1 & Fig. 3 near here>*

227

228 The ELEVATION, BD, DOC, SWC, SAND, SILT, and CLAY were approximately
229 normally distributed, with skewness values of less than 1 (Table 1). Additionally, DOC
230 displayed a moderate CV of 34.6 %, and the other variables had lower CVs (4.1–23.8 %). The
231 NH₄N, NO₃N, SOC and TSN were positively skewed, and the logit-transformations (NH₄Nt,
232 NO₃Nt, SOct and TSnt) had approximately normal distributions (Table1). The NH₄N and
233 NO₃N had very high CVs (190.8 % and 141.6 %, respectively), and the SOC and TSN had
234 moderate CVs (50.1 % and 38.3 %, respectively).

235 The NH₄Nt, NO₃Nt, SOct, TSnt and SWC were significantly correlated with the N₂O fluxes
236 (Fig. 5), and the NH₄Nt, NO₃Nt and TSnt had strong positive relationships with N₂O ($r =$
237 0.71, 0.70 and 0.57, respectively, $p < 0.001$). The N₂O emissions and some soil properties
238 (NH₄N, NO₃N, SOC, TSN and SWC) in the fertilization points were significantly different
239 ($p < 0.001$) from the other three chamber placement positions (Fig. 6). These variables were
240 used as auxiliary covariables for the CK approach.

241

242 <Insert Figs. 4 & 5 near here>

243

244 3.2 Spatial variability of N₂O emissions and related environmental factors

245 Because most of the soil properties were significantly correlated with the chamber placement
246 positions, two types of semivariogram models were calculated for the N₂O and soil
247 parameters (correlated with N₂O fluxes) in the wet season (Table 2). The FLUX30t exhibited
248 strong spatial autocorrelation and was characterized by an exponential semivariogram model,

249 a theoretical distance parameter of 8.40 m (equivalent to an effective range of 25.2 m) and a
250 zero nugget. The NH₄Nt, SWCt, SAND and SILT showed almost no spatial dependency,
251 while NO₃Nt and TSNt demonstrated weak spatial dependency with a range parameter of
252 91.9 and 58.0 m, respectively (equivalent to an effective range of 163.7 and 102.6 m,
253 respectively). The SOCt exhibited a moderate spatial dependency within 93.0 m. By
254 detrending the influence of the chamber placement position, large changes in the
255 semivariogram models occurred regarding the above variables. Although the semivariograms
256 of the regression residuals of FLUX30t, NH₄Nt, NO₃Nt and SOCt were best-fit with the
257 same semivariogram model (exponential) with a similar range of 17.4 m (equivalent to an
258 effective range of 52.1 m), the spatial dependencies of those variables were different (Table
259 2). Of the soil properties, only SOCt had a similar spatial structure to FLUX30t when the
260 influence of the chamber placement position was detrended (Table 2). Based on these
261 correlation analyses and spatial variability analyses, the covariables for the CK method were
262 determined.

263

264 *<Insert Table 2 near here>*

265

266 3.3 Spatial interpolation of N₂O emissions by three methods

267 Three spatial interpolation methods were used in this study to predict the spatial distribution
268 of N₂O emissions from tea soils in the catchment. In the first method, the derived theoretical
269 semivariogram model for FLUX30t that is presented in Table 2 was used for the OK

270 prediction. In the second method, RK was used and the chamber placement position was
271 identified as the auxiliary regression predictor. Thus, the semivariogram of the regression
272 residuals of FLUX30t were calculated and best-fit with the theoretical semivariogram model
273 shown in Fig. 6. In the third method, CK involved two groups of covariables. As described
274 previously, because SOct (detrrending the influence of chamber placement position) showed a
275 similar spatial structure to FLUX30t (detrrending the influence of chamber placing position), a
276 CK process was performed using SOct as the covariable. Firstly, the direct and
277 cross-semivariograms of FLUX30t and SOct (detrrending the influence of the chamber
278 placement position) were calculated and best-fit with a linear model for co-regionalization
279 (LMC). Next, the fitted LMC was used to predict the spatial surface of N₂O emissions.
280 Because NH₄Nt and NO₃Nt were significantly correlated with FLUX30t (Fig. 5), a second
281 CK with NH₄Nt and NO₃Nt as the covariables was processed, similarly to that of the CK
282 with SOct. However, these covariables had different spatial structures (Table 2). As reflected
283 by the lower root mean squared error (RMSE) and higher *r* values (Table 4), the CK method
284 performed better than the other spatial interpolation methods. Furthermore, the CK with
285 NH₄Nt and NO₃Nt as two covariables outperformed the CK with SOct as the covariable.

286

287 *<Insert Figs.6-9 near here>*

288

289 As shown in Fig. 9, the surface map for the spatial distribution of N₂O emissions
290 interpolated by OK was rougher than the maps obtained from the other interpolation

291 approaches. The kriging error maps were showed in Fig. 10, also indicating the CK method
292 outperforming the other spatial interpolation methods. The four kriging interpolations of OK,
293 RK, CK with SOct as the covariable and CK with NH4Nt and NO3Nt as the covariables
294 were able to predict that the total amount of N₂O emissions in the tea fields during the wet
295 season were 208.1 g N d⁻¹, 148.2 g N d⁻¹, 149.7 g N d⁻¹ and 150.5 g N d⁻¹, respectively. From
296 the performance evaluations of the four spatial interpolations, the total N₂O emissions from
297 the tea field on 22 April 2012 during the wet season were approximately 150 g N d⁻¹.

298

299 *<Insert Fig. 10 near here>*

300

301 **Discussion**

302 *4.1 Seasonal differences of N₂O fluxes in the red soil planted with tea*

303 The N₂O emissions from soils have obvious seasonal fluctuations, with emissions that are
304 significantly higher during the wet season than during the dry season (Konda et al., 2010). To
305 understand the seasonal changes in the spatial structures of N₂O fluxes, we compared the
306 N₂O emissions between the wet (this study) and dry (Li et al., 2013) seasons. In general, the
307 mean, SD and coefficient of variation (102.24, 239.96 g N ha⁻¹ d⁻¹ and 234.7 %, respectively)
308 of the N₂O fluxes in the wet season were all higher than those (2.88, 8.94 g N ha⁻¹ d⁻¹ and
309 152.0 %, respectively) during the dry season (Table 3). Furthermore, in contrast with the dry
310 season, the N₂O fluxes during the wet season were significantly different among the four
311 chamber placement positions, with the highest fluxes occurring at the fertilization points and
312 the inter-row positions (Table 3). During the wet season, the high N₂O fluxes at the

313 fertilization points and the inter-row positions resulted from the high soil moisture, due to
314 more rainfall, and from the fertilization that occurred on 19 February 2012 (Fig. 2). The soil
315 N and the soil organic C availability are directly increased by the application of chemical and
316 organic N fertilizers. The additional in the available C and N supplied by fertilization resulted
317 in increased soil microbial activity, which stimulated the nitrification and denitrification
318 processes that contribute to soil N₂O emissions (Davidson et al., 1993; Kiese et al., 2003;
319 Werner et al., 2007).

320

321 *<Insert Table 3 near here>*

322

323 4.2 Spatial structure of N₂O emissions from red soils planted with tea

324 Soil type, topography and land management (fertilization, tillage and irrigation) are the
325 primary factors that affect the spatial structures of N₂O emissions (Folorunso and Rolston,
326 1984; Clemens et al., 1990; Velthof et al., 1996; Konda et al., 2008). During the wet season,
327 the N₂O fluxes showed a strong spatial dependence (with a range of approximately 25.3 m)
328 that was similar to the dry season range of approximately 28.0 m in the tea-planted fields (Li
329 et al., 2013). These results indicated that the spatial dependence of N₂O fluxes at the current
330 spatial sampling scale was comparable between seasons. Our findings for a fertilized tea field
331 were similar to those of Konda et al. (2010) for a tropical forest. However, these results
332 contrasted those of many previous investigations for agricultural fields, including winter
333 wheat (Ball et al., 1997; Clemens et al., 1999; Röver et al., 1999; Mathieu et al., 2006),

334 summer maize (Clements et al., 1999), onion (Yanai et al., 2003), and grassland (Ambus and
335 Christensen, 1994; Velthof et al., 1996; van den Pol-van Dasselaaar et al., 1998; Turner et al.,
336 2008) fields, in which the N₂O flux presented no, weak or moderate spatial dependence. This
337 discrepancy primarily occurred because of the unique geographical characterization and land
338 management of the tea plantation. Compared with other agricultural fields in flat areas, tea
339 fields are always distributed in hills or mountains. Therefore, the contributions of the
340 topography to the spatial dependence of the N₂O flux were strong (Li et al., 2013).
341 Additionally, tea is a perennial plant. Thus, apart from fertilization and weeding, the soil
342 disturbance in tea fields is always very low.

343 During the dry season, the topography (elevation) had a significant effect on the spatial
344 pattern of N₂O fluxes in the tea-planted fields (Li et al., 2013). Similar spatial patterns of N₂O
345 fluxes with topography were also observed in forest soils (Van Kessel et al., 1993; Konda et
346 al., 2010). Theoretically, the SWC varies with the topography and affects the spatial pattern
347 of N₂O fluxes by controlling the conditions for soil nitrification and denitrification (Firestone
348 and Davidson, 1989; Wrage et al., 2004). Although the SWC had no relationships with N₂O
349 and elevation during the dry season (Li et al., 2013), a correlation existed in the present study
350 (Fig. 5). The microstructures of the tea tree-row transect and the land management practices
351 of tea production were the primary influences on the spatial pattern of soil water in the
352 tea-planted fields (Li et al., 2013). During the wet season, fertilization contributed to the
353 spatial pattern of N₂O fluxes in the tea-planted fields, with the highest averaged fluxes at the
354 fertilization sites (198.81 g N ha⁻¹ d⁻¹) (Table 3). Fertilization resulted in similar spatial

355 patterns of N₂O fluxes in other agricultural soils (Ball et al., 1997; Clements et al., 1999;
356 Röver et al., 1999; Mathieu et al., 2006; Yanai et al., 2003).

357 In view of the analysis of the primary factors that affected the spatial pattern of N₂O
358 fluxes, we detrended the influences of the environmental factors when the N₂O flux
359 semivariograms were calculated to more deeply explore the spatial structures of the N₂O
360 emissions in the tea-planted fields. For example, during the dry and wet seasons, the spatial
361 influences of elevation (Li et al., 2013) and chamber placement position, respectively, were
362 detrended when computing the N₂O flux semivariograms. Because the relationship between
363 chamber placement position and N₂O flux was more relevant than the relationship between
364 elevation and N₂O flux, the effect of detrending the influence of chamber placement position
365 during the wet season was more obvious than that of detrending the influence of elevation
366 during the dry season (Li et al., 2013). This effect was also reflected in the evaluation of the
367 performance of the RK method for the wet and dry seasons (Table 4).

368

369 *4.3 Spatial interpolations of N₂O emissions by three methods*

370 The three interpolation methods (OK, RK and CK) were used to predict the spatial
371 distributions of N₂O emissions from the red soils planted with tea during dry (Li et al., 2013)
372 and wet seasons (this study). However, these three methods resulted in significantly different
373 performances between the dry and wet seasons (Table 4). We conducted comparative
374 analyses for the performance of the three interpolation methods using two aspects: different
375 seasons and different methods. Firstly, the OK method performed better when predicting the

376 spatial distribution of N₂O fluxes for the dry season relative to the wet season. Because the
377 OK method directly used the fitted theoretical semivariogram model of the target variable to
378 predict the spatial distribution, its performance reflected the predictive ability of the original
379 data (Goovaerts, 1997). During the wet season, more factors (e.g., NH₄N, NO₃N, SOC, TSN
380 and SWC) influenced the spatial distributions of the N₂O fluxes than the dry season (Table 2
381 and Fig. 5). The values of the original data were concealed. Thus, other sophisticated kriging
382 methods, such as RK and CK, which reconcile the relationships between N₂O fluxes and
383 environmental factors, could be useful. The RK method performed better when elevation was
384 used as an auxiliary regression predictor during the dry season than when the chamber
385 placement position was used during the wet season (Table 4). This finding primarily occurred
386 because the chamber placement position was a categorical variable with a lower regression
387 fitting ability than elevation, which was a continuous variable (Goovaerts, 1997). The
388 performances of the CK with two groups of covariables during the wet season were better
389 than those of the CK with three groups of covariables during the dry season (Table 4).
390 Particularly, the CK with strongly correlated covariables of NO₃N and NH₄N ($r = 0.70-0.71$
391 and $p < 0.001$) (Fig. 5) performed the best ($r = 0.74$ and $RMSE = 1.04$) (Table 4).

392 Secondly, by comparing the performances of the three interpolation methods, the RK and
393 CK methods, which are more sophisticated kriging technologies, performed better than the
394 OK method for the dry and wet seasons. Similar results were obtained by previous
395 researchers (Stein et al., 1988; Odeh et al., 1995; Goovaerts, 1997; Hengl et al., 2004). When
396 comparing the performances of RK and CK, no differences were observed for the dry season.

397 However, during the wet season, the CK significantly outperformed the RK (Table 4). Overall,
398 few attempts have been made to provide a good method for selecting interpolation methods
399 between RK and CK (Kontters et al., 1995; Odeh et al. 1995). Li et al. (2013) suggested that
400 RK was a good choice because of the performance of the two interpolation methods and the
401 difficulties encountered when applying CK. However, in this study, the CK method was
402 better than the RK method because of its high predictive performance (Table 4), its readily
403 available required covariables (e.g., NH₄N, NO₃N and SOC) at co-locations, and because
404 expensive surface data were not needed (e.g., DEM and land use data, which are required by
405 RK) (Goovaerts, 1997; Webster and Oliver, 2001). Our conclusions were similar to those of
406 many previous studies that found that CK was the most versatile and rigorous statistical
407 technique for estimating spatial points (Stein et al., 1988; Odeh et al., 1995; Webster and
408 Oliver, 2001). For the application of CK, the covariables must show a correlation with the
409 target variable and present a similar spatial structure as the target variable (Odeh et al., 1995;
410 Goovaerts, 1997; Webster and Oliver, 2001). Therefore, we further compared the effects of
411 the two groups of covariables for CK in this study. We found that CK method with NH₄Nt
412 and NO₃Nt (showed significant correlations with FLUX30t) as covariables outperformed the
413 CK method with SOCt (presented a similar spatial structure to FLUX30t) as a covariable,
414 indicating that the feature correlation was more important than the similarity of the spatial
415 structure when selecting CK covariables. This finding can be regarded as a prerequisite for
416 selecting covariables for CK application.

417

418

<Insert Table 4 near here>

419

420

421

422

423

424

425

426

427

428

429

430

431

432

433

434

435

The three spatial interpolation methods predicted similar total N₂O emissions from the tea-planted red soils in the 4.0 ha catchment on 30 October 2010 (in the dry season) and on 22 April 2012 (in the wet season), ranging from 21.2 to 22.1 g N d⁻¹ and from 148.2 to 208.1 g N d⁻¹ (Table 4), respectively. The predicted errors during the wet season were higher than those of the dry season (Table 4). This result mainly occurred because fertilization was a major factor that affected the N₂O emissions from the tea fields during the wet season. Following fertilization, the horizontal and vertical movement of NH₄N and NO₃N in the topsoil of the tea fields potentially produced the strong spatial heterogeneity of N₂O emissions. In addition, it is possible that the variations in the availability of oxygen in the soils was regulated by soil moisture, which determined the spatio-temporal heterogeneity of N₂O emissions by inducing different degrees of soil nitrification and denitrification (Davidson et al., 2000; Konda et al., 2010). Thus, spatial interpolation methods must be chosen carefully to accurately estimate the spatial distribution of N₂O emissions when the emissions are high and have strong spatial variability in the fields.

5 Conclusions

436

437

438

During the wet season of 2012, a 30-min one-time measurement of N₂O emissions from a 4.0 ha red-soil tea field in the subtropical region of central China were determined at 147 points. The N₂O fluxes significantly varied with space. In addition, the N₂O fluxes were significantly

439 correlated with the NH₄N, NO₃N, SOC and TSN contents ($r > 0.27$ and $p < 0.001$). The
440 logit-transformed N₂O fluxes demonstrated a strong spatial dependency and were
441 characterized by an exponential semivariogram model with an effective range of 25.2 m.
442 Three spatial interpolation methods (OK, RK and CK) were used to predict the spatial
443 distribution of N₂O emissions. The RK and CK methods were relatively accurate for
444 predicting results. Although the N₂O emissions were much higher during the wet season than
445 in the dry season, the N₂O emissions exhibited similar spatial structure during both seasons.
446 Such a phenomenon was mainly attributed to the low soil disturbance (e.g., only fertilizing
447 in a very small proportion of area and weeding) in the tea field.

448 To effectively mitigate high N₂O emissions from the tea field soils, the biological and
449 chemical mechanisms of N₂O emissions must be deeply explored. In addition, the responsive
450 land management practices, such as biochar application, deep fertilization (under 20 cm), the
451 use of controlled-release fertilizers and ecological engineering, must be recommended and
452 deployed, especially during the wet season.

453

454 **Acknowledgements**

455 The National Basic Research Program of China (2012CB417105) and the National Natural
456 Science Foundation of China (41171200) financially supported this research.

457 **References**

- 458 Akiyama, H., Yan, X. Y., and Yagi, K.: Estimations of emission factors for fertilizer-induced
459 direct N₂O emissions from agricultural soils in Japan: Summary of available data, *Soil Sci.*
460 *Plant Nutr.*, 52, 774-787, 2006.
- 461 Ambus, P. and Christensen, S.: Measurement of N₂O emission from a fertilized grassland: an
462 analysis of spatial variability, *J. Geophys. Res.*, 99, 16557-16567, 1994.
- 463 Armstrong, M.: *Basic linear Geostatistics*, Springer Verlag, Berlin, 153 pp., 1998.
- 464 Ball, B. C., Horgan, G. W., Clayton, H., and Parker, J. P.: Spatial variability of nitrous oxide
465 fluxes and controlling soil and topographic properties, *J. Environ. Qual.*, 26, 1399-1409,
466 1997.
- 467 Clemens, J. Schillinger, M. P., Goldbach, H., and Huwe, B.: Spatial variability of N₂O
468 emissions and soil parameters of an arable silt loam - a field study, *Bio. Fert. Soils*, 28,
469 403-406, 1999.
- 470 Davidson, E. A., Matson, P. A., Vitousek, P. M., Riley, R., Dunkin, K., García-Méndez, G.,
471 and Maass, J. M.: Processes regulating soil emissions of NO and N₂O in a seasonally dry
472 tropical forest, *Ecology*, 74, 130-139, 1993.
- 473 Davidson, E. A., Keller, M., Erickson, H. E., Verchot, L. V., and Veldkamp, E.: Testing a
474 conceptual model of soil emissions of nitrous and nitric oxides, *Bioscience*, 50, 667-680,
475 2000.
- 476 DGUU (Department of Geography, Utrecht University): Introduction for Gstat, available at:
477 <http://www.gstat.org/index.html> (last access: 15 December 2010), 2010.

478 Firestone, M., and Davidson, E.: Microbial basis of NO and N₂O production and
479 consumption, in: Exchange of Trace Gases Between Ecosystems and the Atmosphere,
480 edited by: Andreae, M.O. and Schimel, D.S., John Wiley, Chichester, 7-21, 1989.

481 Folorunso, O. A., and Rolston, D. E.: Spatial variability of field measured denitrification gas
482 fluxes, *Soil Sci. Soc. Am. J.*, 48, 1214-1219, 1984.

483 Fu, X., Li, Y., Xiao, R., Tong, C., and Wu, J.: N₂O emissions from a tea field in subtropical
484 China. In: Proceedings of the 19th World Congress of Soil Science, Soil Solutions for a
485 Changing World, 1–6 August 2010, Brisbane (published on CDROM), 161-163, 2010.

486 Fu, X., Li, Y., Su, W., Shen, J., Xiao, R., Tong, C., and Wu, J.: Annual dynamics of N₂O
487 emissions from a tea field in southern subtropical China, *Plant Soil Environ.*, 58,
488 373-378, 2012.

489 Goovaerts, P.: *Geostatistics for Natural Resources Evaluation*, Oxford University Press, New
490 York, 483 pp., 1997.

491 Gorres, J. H., Dichiario, M. J., and Lyons, J. A.: Spatial and temporal patterns of soil
492 biological activity in a forest and an old field, *Soil Biol. Biochem.*, 30, 219-230, 1998.

493 Han, W. Y., Xu, J. M., Wei, K., Shi, W. Z., and Ma, L. F.: Estimation of N₂O emission from
494 tea garden soils, their adjacent vegetable garden and forest soils in eastern China, *Environ.*
495 *Earth Sci.*, 70, 2495-2500, 2013.

496 Hayatsu, M.: The lowest limit of pH for nitrification in tea soil and isolation of an acidophilic
497 ammonia oxidizing bacterium, *Soil. Sci. Plant Nutr.*, 39, 219-226, 1993.

498 Hengl, T., Heuvelink, G. B. M., and Stein, A.: A generic framework for spatial prediction of
499 soil variables based on regression-kriging, *Geoderma*, 120, 75-93, 2004.

500 Hirono, Y., and Nonaka, K.: Nitrous oxide emissions from green tea fields in Japan:
501 contribution of emissions from soil between rows and soil under the canopy of tea plants,
502 *Soil. Sci. Plant Nutr.*, 58, 384-392, 2012.

503 IPCC: Climate change 2013: the physical science basis. Contribution of working group I, in:
504 Fourth assessment report of the intergovernmental panel on climate change, edited by:
505 Solomon S., Qin D., Manning, M., Chen Z., Marquis, M., Averyt, K.B., Tignor, M.,
506 Miller, H.L., Cambridge University Press, Cambridge, 996 pp., 2013.

507 ISM (Institute for Statistics and Mathematics): The R Project for Statistical Computing,
508 available at: <http://www.r-project.org/> (last access: 15 December 2010), 2010.

509 Kiese, R., Hewett, B., Graham, A., and Butterbach-Bahl, K.: Seasonal variability of N₂O
510 emissions and CH₄ uptake by tropical rainforest soils of Queensland, Australia. *Global*
511 *Biogeochem. Cy.*, 17, 1043, doi:10. 1029/2002GB002014, 2003.

512 Konda, R., Ohta, S., Ishizuka, S., Arai, S., Ansori, S., Tanaka, N., and Hardjono, A.: Spatial
513 structures of N₂O, CO₂, and CH₄ fluxes from *Acacia mangium* plantation soils during a
514 relatively dry season in Indonesia, *Soil Biol. Biochem.*, 40, 3021-3030, 2008.

515 Konda, R., Ohta, S., Ishizuka, S., Heriyanto, J., and Wicaksono, A.: Seasonal changes in the
516 spatial structures of N₂O, CO₂ and CH₄ fluxes from *Acacia mangium* plantation soils in
517 Indonesia, *Soil Biol. Biochem.*, 42, 1512-1522, 2010.

518 Li, Y., Fu, X., Liu, X., Shen, J., Luo, Q., Xiao, R., Li, Y., Tong, C., and Wu, J.: Spatial
519 variability and distribution of N₂O emissions from a tea field during the dry season in
520 subtropical central China, *Geoderma*, 193, 1-12, 2013.

521 Lin, Y., and Han, W.: N₂O emissions from different soils, *Chinese Journal of Tea Science*, 29,
522 456-464, 2009.

523 Mathieu, O., Lévêque, J., Hénault, C., Milloux, M. J., Bizouard, F., and Andreux, F.:
524 Emissions and spatial variability of N₂O, N₂ and nitrous oxide mole fraction at the field
525 scale, revealed with ¹⁵N isotopic techniques, *Soil Biol. Biochem.*, 38, 941-951, 2006.

526 Meda, B., Flechard, C. R., Germain, K., Robin, P., Walter, C., and Hassouna, M.:
527 Greenhouse gas emissions from the grassy outdoor run of organic broilers,
528 *Biogeosciences*, 9, 1493-1508, doi:10.5194/bg-9-1493-2012, 2012.

529 Mosier, A. R., Duxbury, J. M., Freney, J. R., Heinemeyer, O., and Minami, K.: Nitrous oxide
530 emissions from agricultural fields: assessment, measurement and mitigation. *Plant Soil*,
531 181, 95-181, 1996.

532 Mosier, A. R., Kroeze, C., Nevison, C., Oenema, O., Seitzinger, S., and van Cleemput, O.:
533 Closing the global N₂O budget: nitrous oxide emissions through the agricultural nitrogen
534 cycle, *Nutr. Cycl. Agroecosys.*, 52, 225-248, 1998.

535 NBSC (a): China Statistical Yearbook, annual publication, National Bureau of Statistics of
536 China, Beijing, 2014.

537 Odeh, I. O. A., McBratney, A. B., and Chittleborough, D. J.: Spatial prediction of soil
538 properties from landform attributes derived from a digital elevation model, *Geoderma*, 63,
539 197-214, 1994.

540 Odeh, I. O. A., McBratney, A. B., and Chittleborough, D. J.: Further results on prediction of
541 soil properties from terrain attributes: heterotopic cokriging and regression kriging,
542 *Geoderma*, 67, 215-226, 1995.

543 R Development Core Team: R: a language and environment for statistical computing. R
544 Foundation for Statistical Computing, 2014.

545 Ravishankara, A. R., Daniel, J. S., and Portmann, R. W.: Nitrous oxide (N₂O): the dominant
546 ozone-depleting substance emitted in the 21st century, *Science*, 326, 123-125, 2009.

547 Röver, M., Heinemeyer, O., Munch, J. C., and Kaiser, E. A.: Spatial heterogeneity within the
548 plough layer: high variability of N₂O emission rates, *Soil Biol. Biochem.*, 31, 167-173,
549 1999.

550 Stein, A., van Dooremolen, W., Bouma, J., and Bregt, A. K.: Cokriging point data on
551 moisture deficit. *Soil Sci. Soc. Am. J.*, 52, 1418-1423, 1988.

552 Tokuda, S. I., and Hayatsu, M.: Nitrous oxide flux from a large amount of nitrogen fertilizer
553 and soil environmental factors controlling the flux, *Soil. Sci. Plant Nutr.*, 50, 365-374,
554 2004.

555 Turner, D. A., Chen, D., Gellbally, I. E., Li, Y., Edis, R. B., Leuning, R., Kelly, K., and
556 Phillips, F.: Spatial variability of nitrous oxide emissions from an Australian irrigated
557 dairy pasture, *Plant soil*, 309, 77-88, 2008.

558 Van den Pol-van Dasselaar, A., Corré, W. J., Klemedtsson, A., Weslien, P., Stein, A.,
559 Klemedtsson, L., and Oenema, O.: Spatial variability of methane, nitrous oxide, and
560 carbon dioxide emissions from drained grasslands, *Soil Sci. Soc. Am. J.*, 62, 810-817,
561 1998.

562 Van Kessel, C., Pennock, D.J., and Farrell, R.E.: Seasonal-variations in denitrification and
563 nitrous oxide evolution at the landscape scale, *Soil Sci. Soc. Am. J.*, 57, 988-995, 1993.

564 Velthof, G. L., Jarvis, S. C., Stein, A., Allen, A. G., and Oenema, O.: Spatial variability of
565 nitrous oxide fluxes in mown and grazed grasslands on a poorly drained clay soil, *Soil*
566 *Biol. Biochem.*, 28, 1215-1225, 1996.

567 Venterea, R. T., and Rolston, D. E.: Mechanisms and kinetics of nitric and nitrous oxide
568 production during nitrification in agricultural soil, *Glob. Change Biol.*, 6, 303-316, 2000.

569 Webster, R.: Quantitative spatial analysis of soil in the field, in: *Advances in Soil Science*,
570 edited by: Stewart, B.A., Springer, New York, 1-70, 1985.

571 Webster, R., and Oliver, M. A.: *Geostatistics for Environmental Scientists*, John Wiley &
572 Sons, Chichester, 2001.

573 Werner, C., Kiese, R., and Butterbach-Bahl, K.: Soil-atmosphere exchange of N₂O, CH₄, and
574 CO₂ and controlling environmental factors for tropical rain forest sites in western Kenya,
575 *J. Geophys Res.*, 112, D03308, doi:10.1029/2006JD007388, 2007.

576 Wrage, N., Velthof, G. L., Laanbroek, H. J., and Oenema, O.: Nitrous oxide production in
577 grassland soils: assessing the contribution of nitrifier denitrification, *Soil Biol. Biochem.*,
578 36, 229-236, 2004.

579 Yanai, J., Lee, C. K., Umeda, M., and Kosaki, T.: Spatial variability of soil chemical
580 properties in a paddy field. *Soil Sci. Plant Nutr.*, 46, 473-482, 2000.

581 Yanai, J., Sawamoto, T., Oe, T., Kusa, K., Yamakawa, K., Sakamoto, K., Naganawa, T.,
582 Inubushi, K., Hatano, R., and Kosaki, T.: Atmospheric pollutants and trace gases: spatial
583 variability of nitrous oxide emissions and their soil-related determining factors in an
584 agricultural field, *J. Environ. Qual.*, 32, 1965-1977, 2003.

585

586 Table 1 Descriptive statistics of the N₂O fluxes and environmental factors.

Variable ^a	Mean	Minimum	Maximum	CV (%)	Skewness of the original data	Skewness of the logit-transformed data
FLUX30	102.24 ^b	-1.73	1,659.11	234.7	4.37	0.6
ELEVATION	80.64	74.25	87.96	4.1	0.04	-
BD	1.26	0.90	1.56	10.1	-0.28	-
DOC	185.56	43.70	424.14	34.6	0.75	-
NH4N	62.33	1.89	842.55	190.8	3.28	0.17
NO3N	21.54	0.48	135.29	141.6	1.85	0.28
SOC	13.33	5.11	52.52	50.1	2.27	-0.44
TSN	1.52	0.81	4.12	38.3	1.73	-0.01
SWC	0.33	0.19	0.47	16.6	0.07	-
SAND	39.73	16.98	63.79	23.8	0.02	-
SILT	47.15	26.78	64.17	16.1	-0.29	-
CLAY	13.12	8.68	21.68	21.5	1.00	-

587 ^a FLUX30 is the N₂O flux (g N ha⁻¹ d⁻¹); ELEVATION is the elevation (m); and BD, DOC,
588 NH4N, NO3N, SOC, TSN, SWC, SAND, SILT and CLAY are the soil bulk density (Mg m⁻³),
589 soil dissolved organic carbon (mg C kg⁻¹ soil), soil ammonium (mg N kg⁻¹ soil), soil nitrate
590 (mg N kg⁻¹ soil), soil organic carbon (g C kg⁻¹ soil), soil total nitrogen (g N kg⁻¹ soil),

591 gravimetric soil water ($\text{g H}_2\text{O g}^{-1}$ soil), soil sand particle (%), soil silt particle (%) and soil
592 clay particle (%) content, respectively, of the 0-20 cm of topsoil.

593 ^b The median and standard deviation of the FLUX30 were 27.56 and 239.96 $\text{g N ha}^{-1} \text{d}^{-1}$,
594 respectively.

595 Table 2 Semivariogram models for N₂O fluxes and the environmental factors.

Variable	Model	Nugget	Partial sill	Sill(nugget+ partial sill)	Distance Parameter (m)	Effective range (m)	Partial sill/sill
FLUX30t ^a	Exp	0	3.7186	3.7186	8.40	25.2	1.00
NH4Nt ^a	ND ^c	ND ^c	ND ^c	ND ^c	ND ^c	ND ^c	ND ^c
NO3Nt ^a	Ste	4.0794	0.6113	4.6907	91.92	163.7	0.13
SOct ^a	Sph	1.1198	0.7744	1.8942	92.96	93.0	0.41
TSNt ^a	Ste	1.0422	0.2816	1.3238	57.97	102.6	0.21
SWCt ^a	ND ^c	ND ^c	ND ^c	ND ^c	ND ^c	ND ^c	ND ^c
SAND ^a	ND ^c	ND ^c	ND ^c	ND ^c	ND ^c	ND ^c	ND ^c
SILT ^a	ND ^c	ND ^c	ND ^c	ND ^c	ND ^c	ND ^c	ND ^c
FLUX30t ^b	Exp	1.1911	2.0560	3.2471	17.36	52.1	0.63
NH4Nt ^b	Exp	2.0473	0.7185	2.7658	17.36	52.1	0.26
NO3Nt ^b	Exp	1.6241	1.1188	2.7429	17.36	52.1	0.41
SOct ^b	Exp	0.6043	1.0777	1.6820	17.36	52.1	0.64
TSNt ^b	Ste	0.9347	0.3114	1.2461	59.53	105.4	0.25
SWCt ^b	ND ^c	ND ^c	ND ^c	ND ^c	ND ^c	ND ^c	ND ^c
SAND ^b	ND	ND	ND	ND	ND	ND	ND
SILT ^b	ND	ND	ND	ND	ND	ND	ND

596 ND, not determined.

597 ^a Semivariogram models for the OK method.

598 ^b Semivariogram models for the RK method using the chamber placement position as the

599 auxiliary regression predictor.

600 ^c Spatial structures were not apparent.

601 Table 3 Statistics for N₂O fluxes during the dry and wet seasons.

Sample position	Mean	SD	Median	Max.	Min.	CV (%)
Dry season						
Inter-row (58)	5.15	4.95	4.09	22.43	-2.83	96.1
Fertilization point (50)	7.19	12.04	4.34	79.56	-6.42	167.4
Under tree (28)	3.58	2.91	2.36	10.28	0.68	81.3
In tree row (11)	5.95	10.38	3.98	52.17	-5.69	174.5
Wet season						
Inter-row (45)	101.69	287.23	27.56	1,659.11	-0.81	282.5
Fertilization point (45)	198.81	295.70	73.42	1,404.32	0.85	148.7
Under tree (22)	16.74	17.00	10.64	61.24	-1.73	101.6
In tree row (33)	28.30	38.34	14.72	177.08	0.19	135.5

602

603 The numbers in the parentheses represent the sample numbers for each chamber placement
 604 position.

605 Table 4 Cross-validations of the three different kriging interpolations for N₂O fluxes during
 606 the dry and wet seasons.

Method of spatial interpolation	Auxiliary variable	ME (no dimension)	RMSE (no dimension)	<i>r</i>	Predicted total N ₂ O emissions (g N d ⁻¹)
Dry season					
OK	-	0.0002	0.102	0.52	22.1 ^a
RK	ELEVATION	0.0008	0.098	0.57	21.1 ^a
CK	SOct	0.0006	0.103	0.51	22.0 ^a
CK	ELEV	0.0008	0.099	0.57	21.5 ^a
CK	SOct and ELEV	0.0009	0.098	0.57	21.2 ^a
Wet season					
OK	-	-0.0005	1.739	0.18	208.1
RK	POSITION	-0.0006	1.549	0.49	148.2
CK	SOct (POSITION)	0.0020	1.439	0.58	149.5
CK	NH4Nt (POSITION) and NO3Nt (POSITION)	0.0001	1.185	0.74	150.5

607 OK, RK and CK correspond to ordinary kriging, regression kriging and cokriging,
608 respectively; For the dry season campaign, ELEVATION, SOct and ELEV are the normalized
609 elevation, the normalized soil organic carbon content and the inverse of the normalized
610 elevation, respectively. For the wet season campaign, SOct, NH4Nt and NO3Nt are the
611 logit-transformations of soil organic carbon, soil ammonium and soil nitrate concentrations,
612 respectively. "POSITION" (in the parentheses) indicates the process of detrending the
613 influence of chamber placement position. The ME, RMSE, and r are the mean prediction
614 error, the root mean squared error (the mean squared deviation ratio of the prediction
615 residuals to the kriging standard errors), and the Pearson's correlation coefficient between the
616 observations and the predictions, respectively.

617 ^aThe predicted total N₂O emissions during the dry season were recalculated because the
618 study area changed from 4.8 ha to 4.0 ha for the wet season.

619 **Figure captions**

620

621 Figure 1. **(a, b)** Location and **(c, d)** digital elevation model and land use map of the tea
622 planted catchment. The red circles in **(c, d)** represent the sample points. The catchment is
623 located in Jinjing town, which is 70 km northeast of Changsha, the capital city of Hunan
624 Province, China.

625

626 Figure 2. Daily **(a)** air temperatures and **(b)** precipitation during 2012.

627

628 Figure 3. Histograms of **(a)** the original N₂O fluxes (FLUX30) and **(b)** the logit-transformed
629 N₂O fluxes (FLUX30t).

630

631 Figure 4. The Tukey's Honest Significant Difference analysis for FLUX30t, NH₄Nt, NO₃Nt,
632 SO₄t, TSNt and SWCt based on the four-chamber placement positions (R, inter-row; F,
633 fertilization point; U, under tea tree; and I, in the tea tree row).

634

635 Figure 5. Correlation matrix with the Pearson's correlation coefficients (r) of the N₂O fluxes
636 and the environmental factors. All of the variables in the correlation matrix are normally
637 distributed. FLUX30 represents the N₂O flux (g N ha⁻¹ d⁻¹); ELEVATION is the elevation (m);
638 and BD, DOC, NH₄N, NO₃N, SOC, TSN, SWC, SAND, SILT and CLAY are the soil bulk
639 density (Mg m⁻³), soil dissolved organic carbon (mg C kg⁻¹ soil), soil ammonium (mg N kg⁻¹

640 soil), soil nitrate (mg N kg^{-1} soil), soil organic carbon (g C kg^{-1} soil), total soil nitrogen (g N
641 kg^{-1} soil), gravimetric soil water ($\text{g H}_2\text{O g}^{-1}$ soil), soil sand particle (%), soil silt particle (%)
642 and soil clay particle (%) contents of the top 0-20 cm of the soil, respectively. Furthermore, *,
643 ** and *** represent the statistical significance at probability levels of 0.05, 0.01 and 0.001,
644 respectively. The lowercase letter t represents the logit transformation.

645

646 Figure 6. Semivariograms (open circles) and best-fitted models (solid lines) of the normal
647 logit-transformed N_2O fluxes (FLUX30t) (no dimension) for ordinary kriging (**a**) and the
648 regression residuals of FLUX30t (no dimension) with chamber placement position as the
649 predictor for regression kriging (**b**).

650

651 Figure 7. Direct and cross-semivariograms (open circles, detrending the influence of chamber
652 placement position for cokriging) and the best-fitted linear model of the co-regionalization
653 (solid lines) of the normal logit-transformed N_2O fluxes (FLUX30t) (no dimension) and the
654 normal SOC (SOCt, no dimension). The linear model of co-regionalization was characterized
655 by using the same range and different sills for its component models.

656

657 Figure 8. Direct and cross-semivariograms (open circles, detrending the influence of chamber
658 placement position for cokriging) and the best-fit linear model of co-regionalization (solid
659 lines) for the normal logit-transformed N_2O fluxes (FLUX30t) (no dimension), NH_4N
660 (NH_4Nt , no dimension) and NO_3N (NO_3Nt , no dimension). The linear model of

661 co-regionalization was characterized by the same range and different sills for its component
662 models.

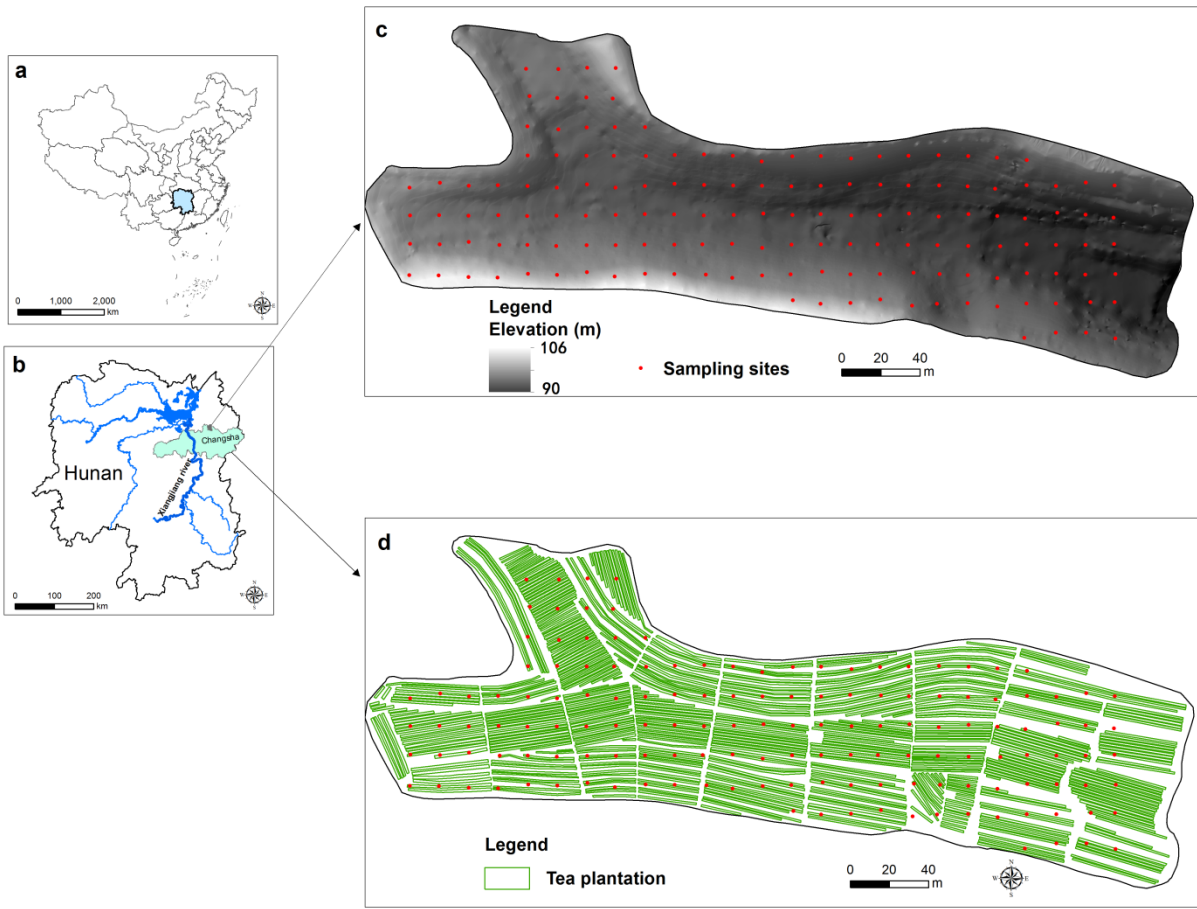
663

664 Figure 9. Spatial distributions of the N₂O fluxes as predicted by **(a)** OK, **(b)** RK with
665 chamber placement position as the regression predictor, **(c)** CK with SOct (with the influence
666 of chamber placement position detrended) as the covariable, and **(d)** CK with NH₄Nt (with
667 the influence of chamber placement position detrended) and NO₃Nt (with the influence of
668 chamber placement position detrended) as two covariables. Here, SOct, NH₄Nt and NO₃Nt
669 represent the logit-transformed soil organic carbon, soil ammonium and soil nitrate content,
670 respectively.

671

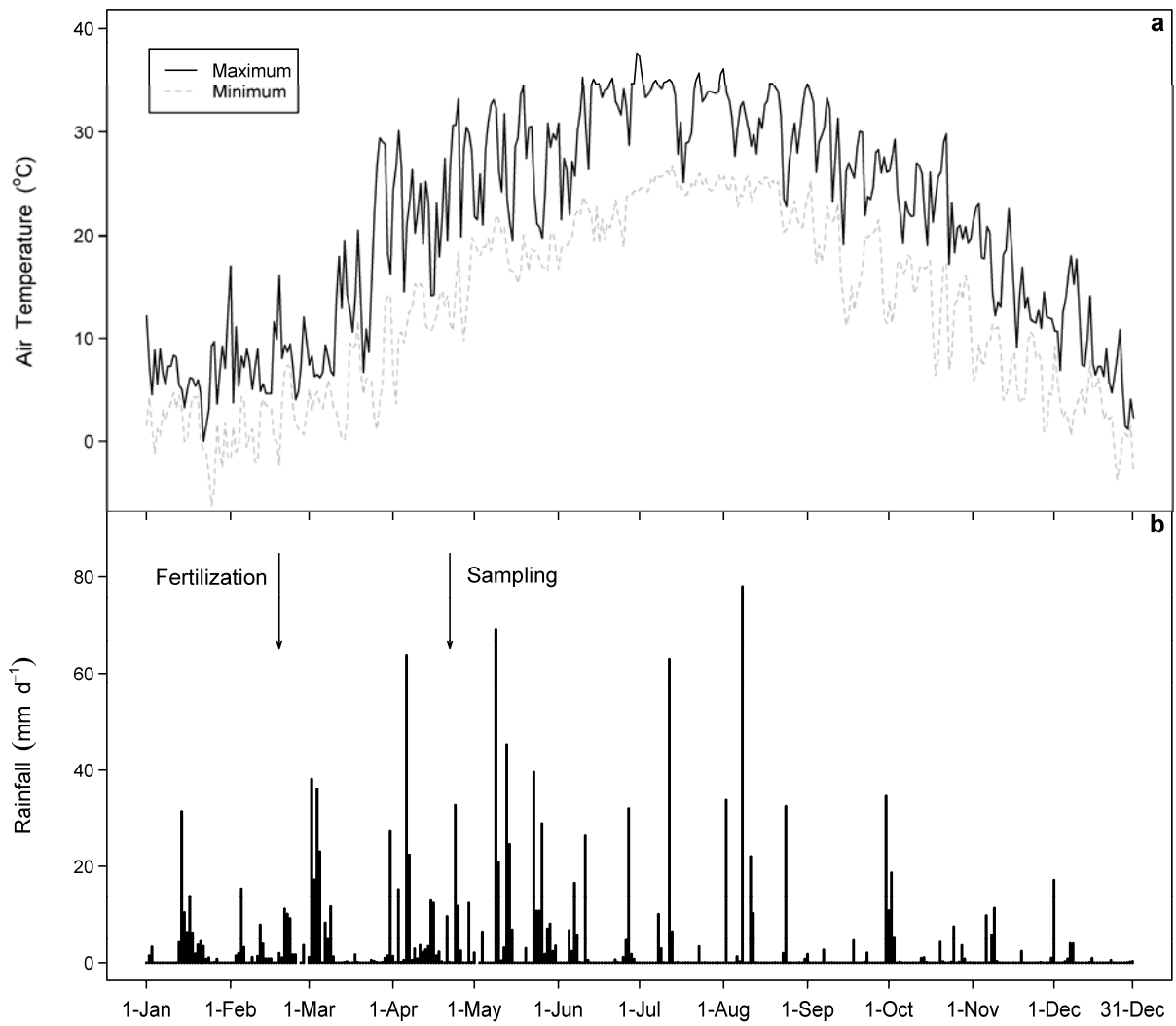
672 Figure 10. Spatial distributions of kriging variance of the N₂O fluxes as predicted by **(a)** OK,
673 **(b)** RK with chamber placement position as the regression predictor, **(c)** CK with SOct (with
674 the influence of chamber placement position detrended) as the covariable, and **(d)** CK with
675 NH₄Nt (with the influence of chamber placement position detrended) and NO₃Nt (with the
676 influence of chamber placement position detrended) as two covariables. Here, SOct, NH₄Nt
677 and NO₃Nt represent the logit-transformed soil organic carbon, soil ammonium and soil
678 nitrate content, respectively.

679



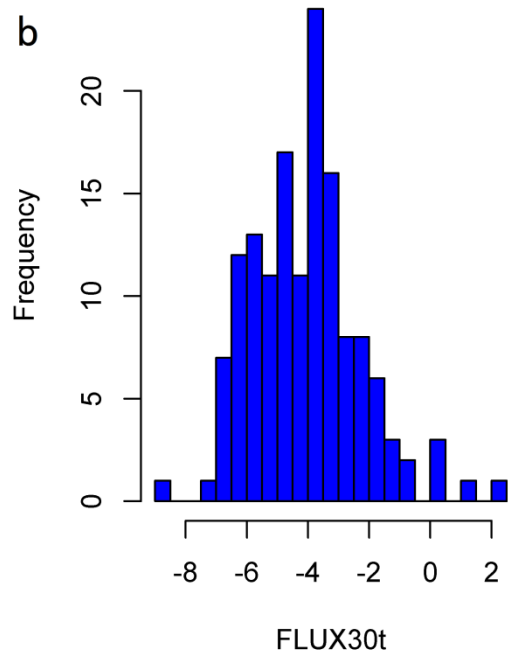
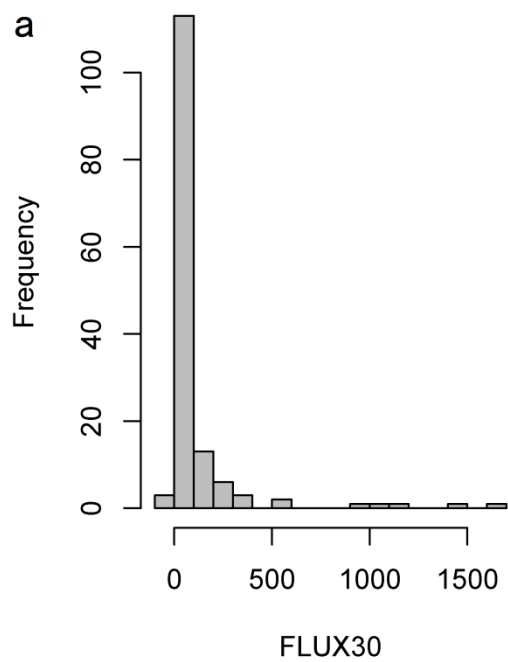
680

681 Figure 1



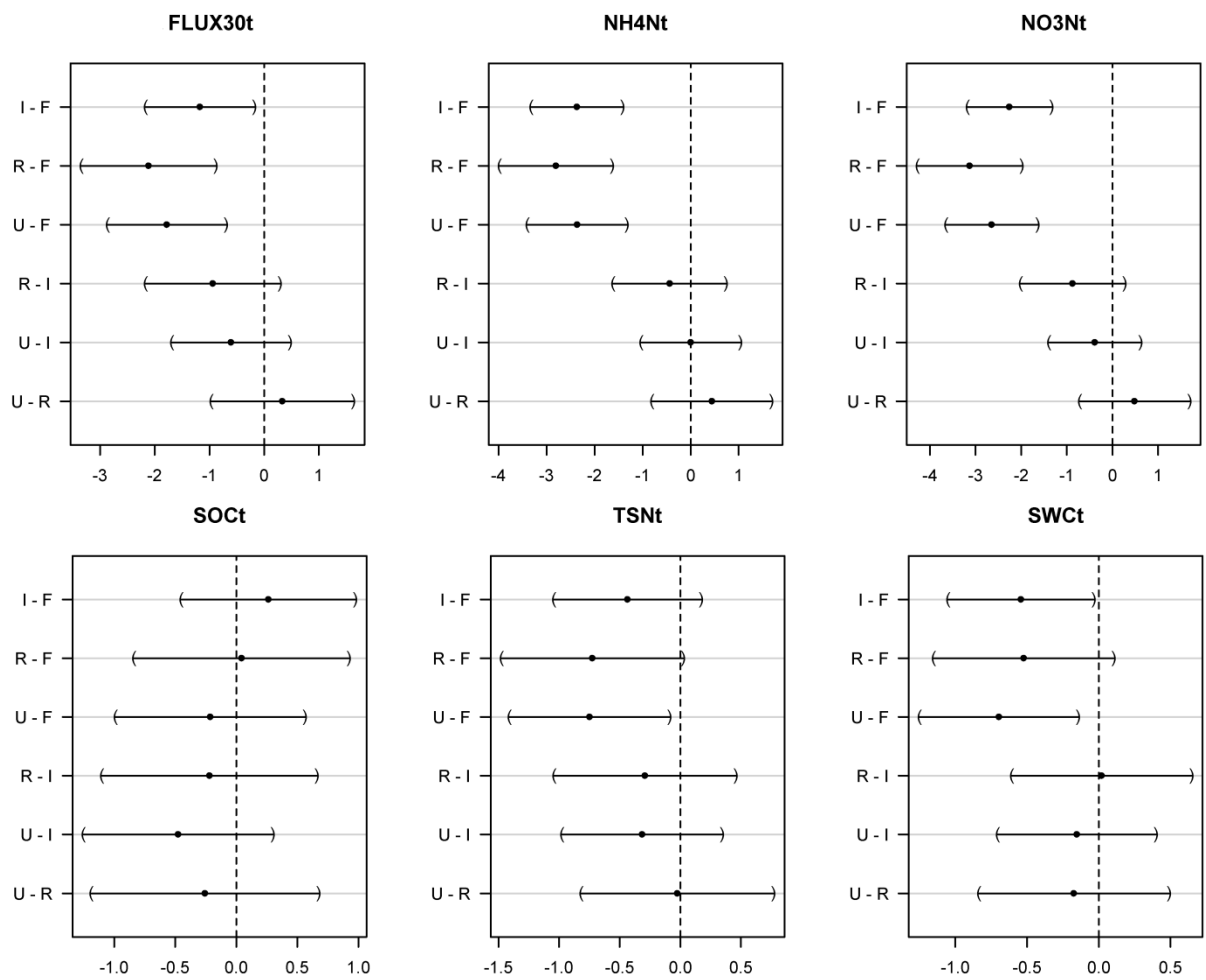
682

683 Figure 2



684

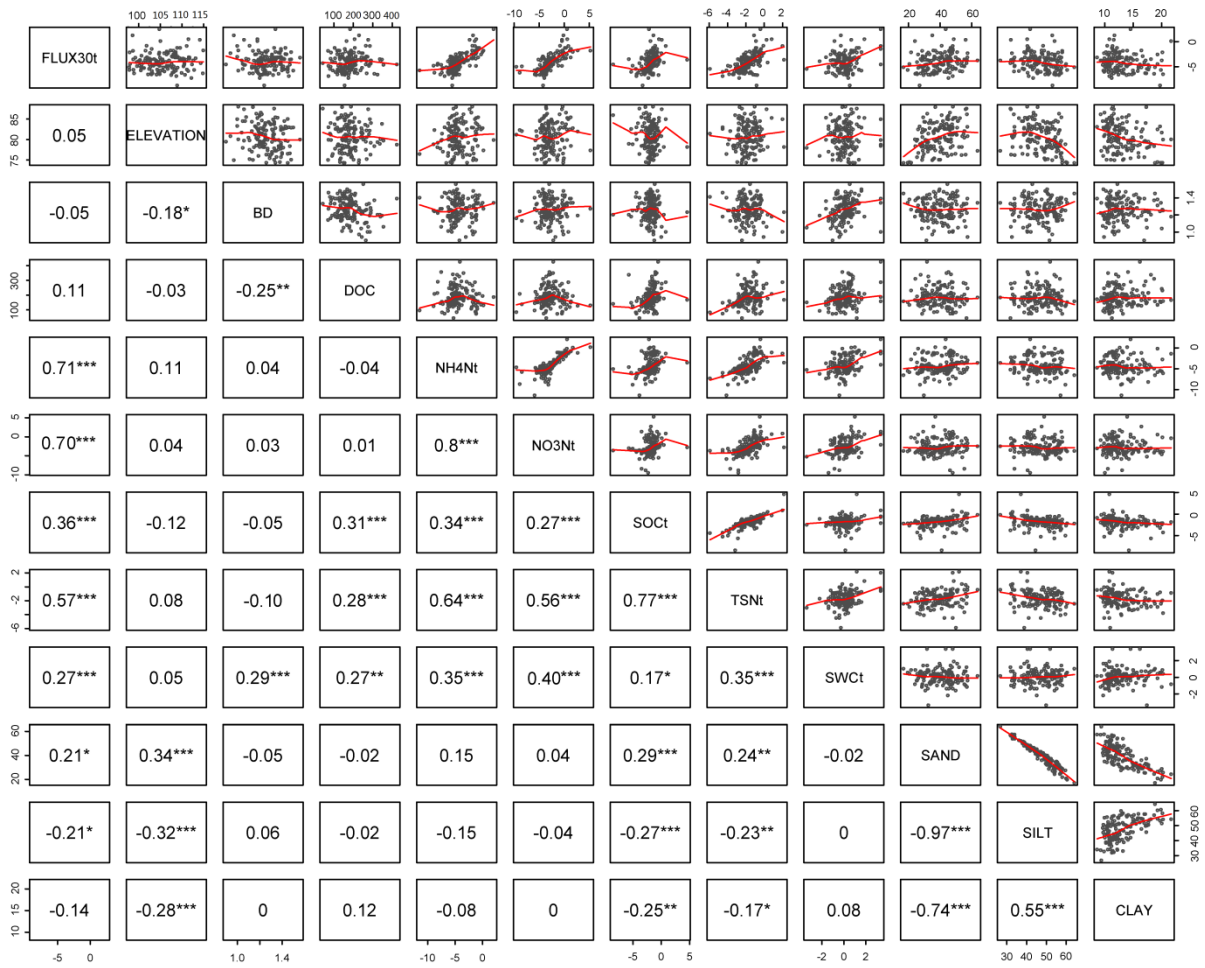
685 Figure 3



686

687 Figure 4

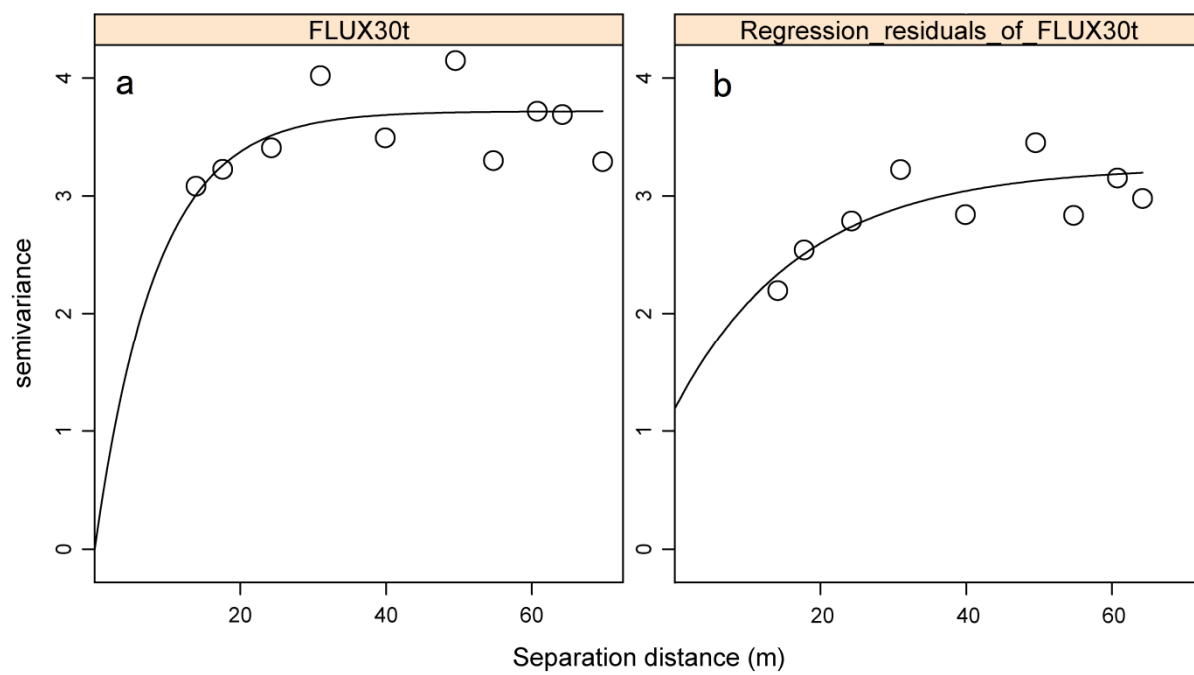
688



689

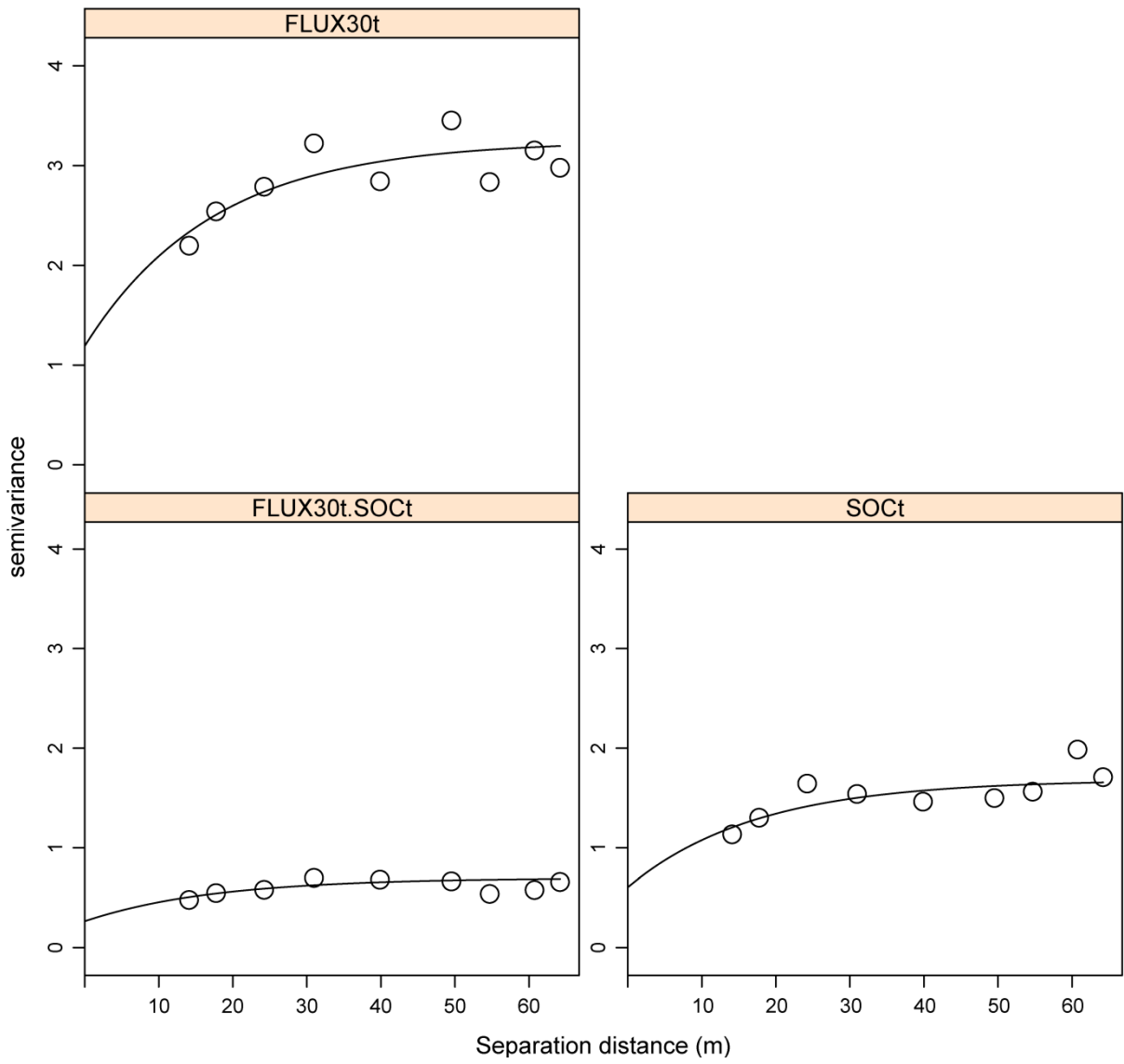
690 Figure 5

691



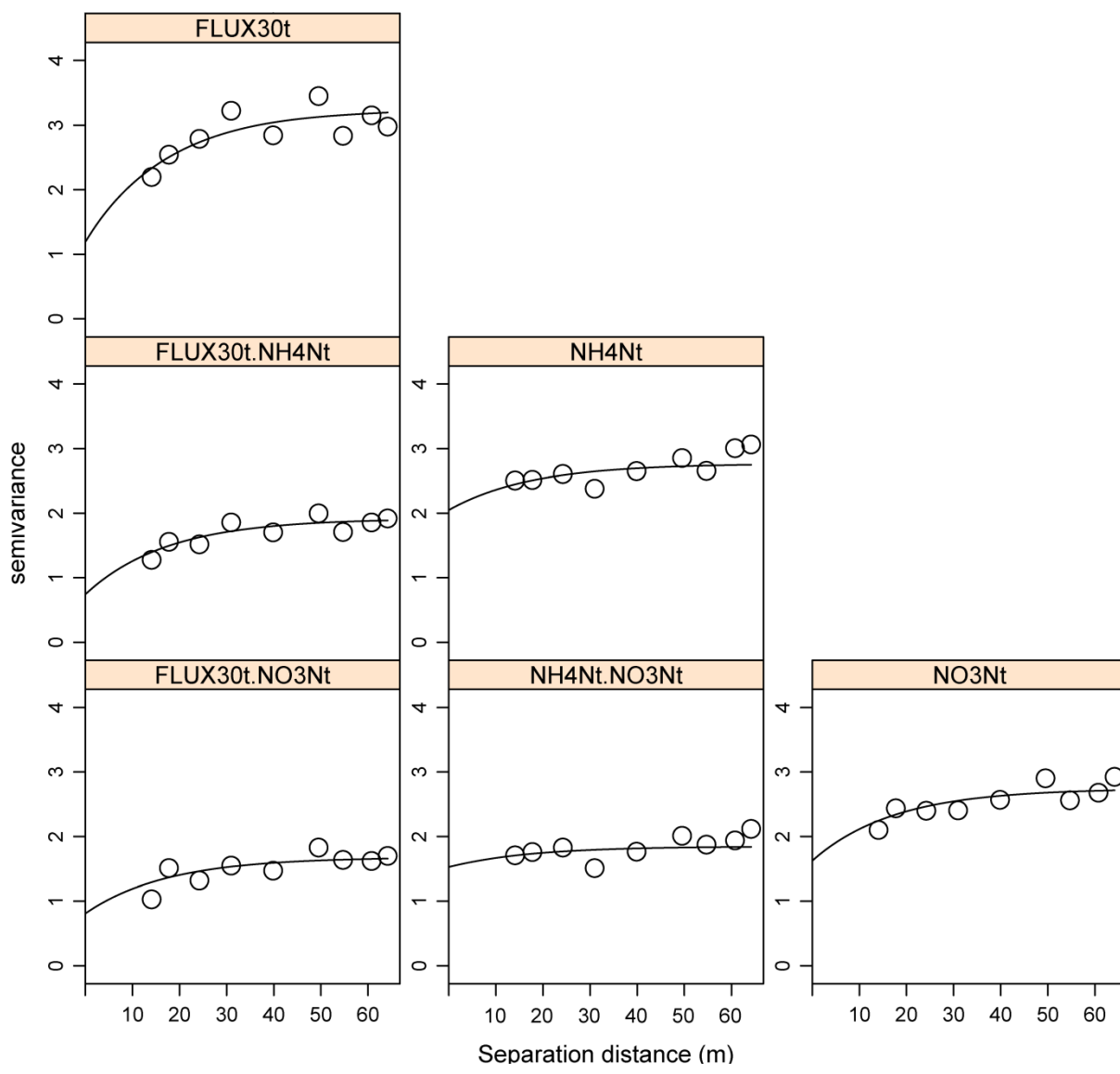
692

693 Figure 6



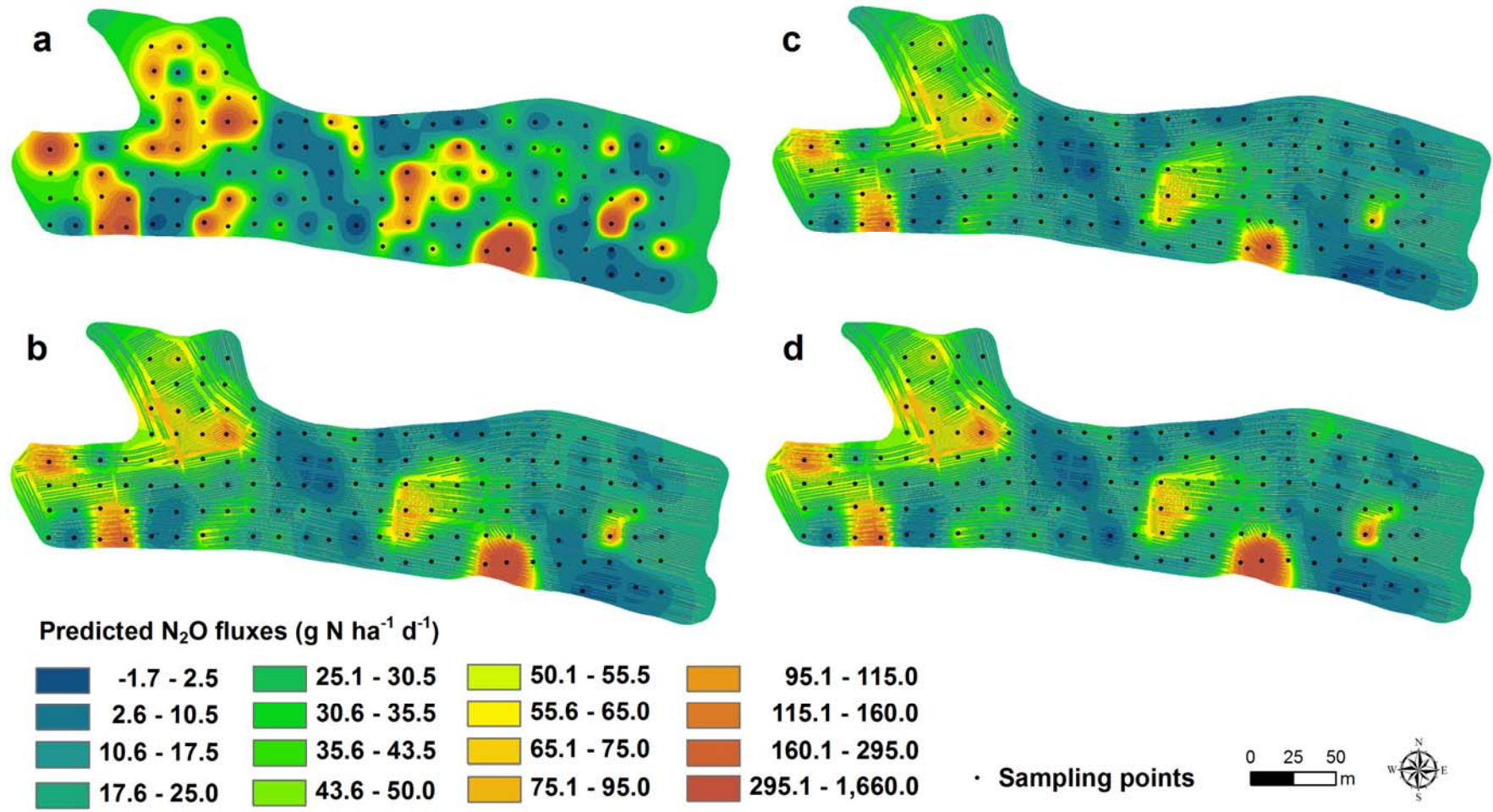
694
 695
 696
 697

Figure 7



698

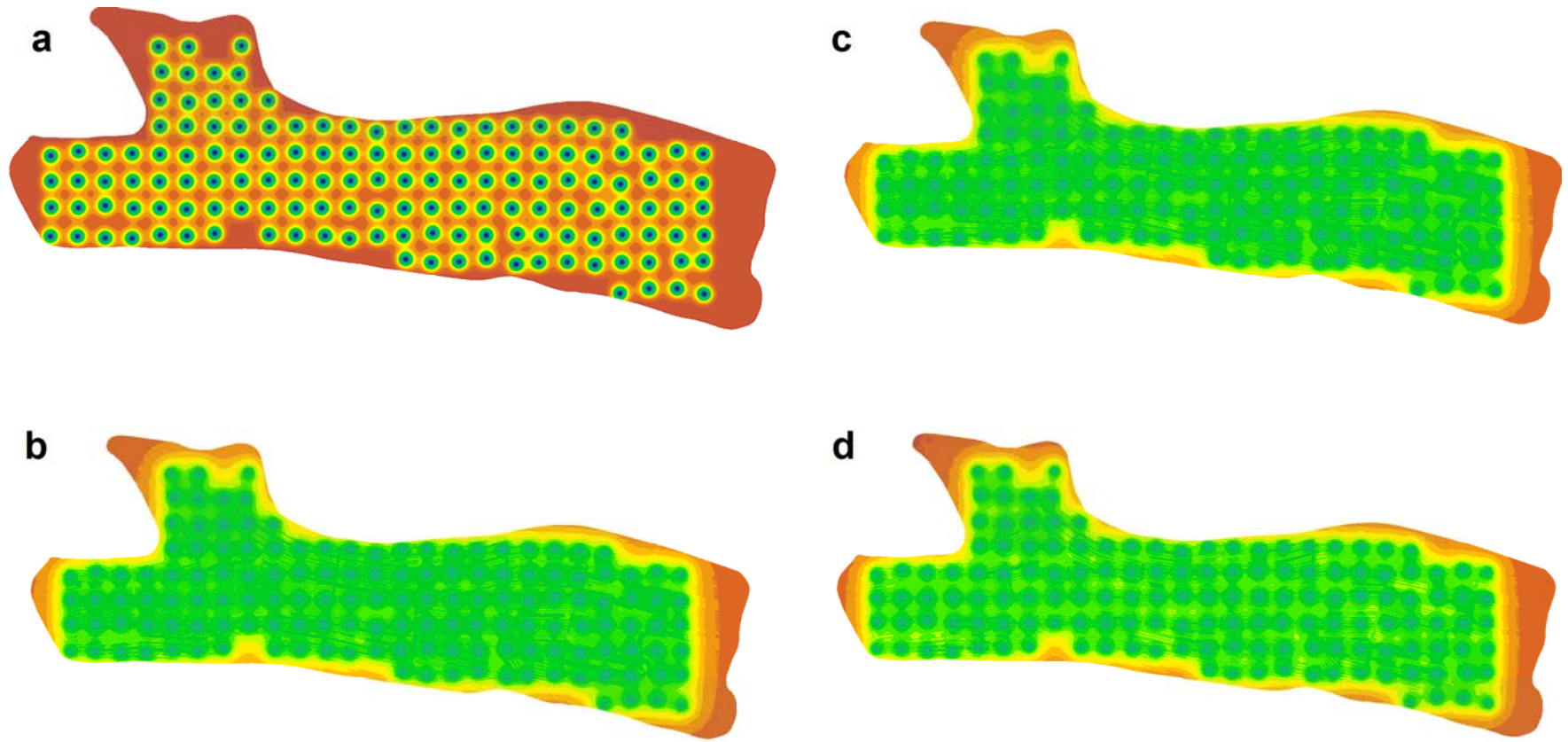
699 Figure 8



700

701 Figure 9

702



Kriging variance



703

704

705

Figure 10